CERN – EUROPEAN ORGANIZATION FOR NUCLEAR RESEARCH

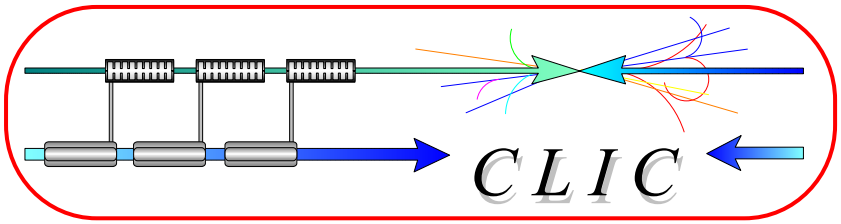

CLIC Note 547

CERN-OPEN-2002-072
19/11/2002

DIFFRACTION RADIATION ANGULAR SPECTRAL DISTRIBUTIONS

J. Bosser, G. Tranquille

Abstract

In a previous paper we have shown that, when applied to CLIC type beams, diffraction radiation (DR) should provide enough photons in the visible range to allow diagnostics measurements of the particle beam. In the present note we analyze in detail the horizontal and vertical polarization component distributions. Special emphasis is given to the influence of the electron beam r.m.s width and divergence.

Geneva, Switzerland
19/11/2002

DIFFRACTION RADIATION. ANGULAR SPECTRAL DISTRIBUTIONS

1. Introduction

In a previous paper [1] we have shown that, when applied to CLIC type beams, diffraction radiation (DR) should provide enough photons in the visible range to allow diagnostics measurements of the particle beam. In the present note we analyze in detail the horizontal and vertical polarization component distributions. Special emphasis is given to the influence of the electron beam r.m.s width and divergence.

2. Symbols and Data

We refer to Figure 1 in which some of the symbols used are shown.
The unit ortho-normal vectors are defined by: $\vec{e}_x, \vec{e}_y, \vec{e}_z$ as shown in Figure 1.c.

The actual slit orientation could be rotated by 90^o but the main issues of our analysis would remain the same. Here we consider only the backward radiation from a perfectly conducting foil.

The particle has its nominal velocity directed along the x axis and is offset by "δ" as shown in Figure1.a. Taking into account the transverse components we can write the velocity as follows: $\vec{v} = v_x\vec{e}_x + v_y\vec{e}_y + v_z\vec{e}_z$, with $|v_y| << v_x$ and $|v_z| << v_x$ such that the relativistic factors can be defined by:

$$\beta = \frac{v}{c} \cong \frac{v_x}{c} \text{ and } \gamma = \frac{1}{\sqrt{1-\beta^2}}$$, the γ factor is assumed to be large.

The plane of incidence is formed by the nominal velocity vector $\vec{v}$ and the normal to the reflecting plane $\vec{n}$ (Fig.1.b). The slit is thus parallel to the plane of incidence.

The emitted photon wave vector $\vec{k}$ is primarily directed along the $\vec{e}_z$ axis and defined as follows:

$$\left|\vec{k}\right| = \frac{\omega}{c} = \frac{2\cdot\pi}{\lambda} = \frac{1}{\bar{\lambda}}$$

In the $(\vec{e}_x, \vec{e}_y)$ plane the wave vector components are:

$$k_x = k\cdot\sin(\theta_x), \quad k_y = k\cdot\sin(\theta_y)$$

with: $\theta_{x,y}$ the projected angle of the vector $\vec{k}$ onto the (x,z) and (y,z) planes, respectively (Figure 1.c).

3. Horizontal and Vertical Components.

The emitted photons are polarized. We can therefore consider:

- The horizontally polarized intensity which is parallel to the slit edge,
- The vertically polarized intensity which is perpendicular to the slit edge.

We use the limiting forms for backward DR at 45° as described in reference [2].

Each component can be expressed as follows:

$$\frac{d^2N_{horriz}}{d\omega d\Omega} = |r_\sigma|^2 \frac{\alpha}{4\cdot\pi^2\cdot\omega}\gamma^2 \frac{X^2}{1+X^2}\frac{e^{-R\cdot(1+X^2)^{1/2}}}{1+X^2+Y^2}\cdot[\cosh(2\cdot f\cdot\delta)+\sin(R\cdot Y+\Phi'(X,Y)]$$

$$\frac{d^2N_{vert}}{d\omega d\Omega} = |r_\perp|^2 \frac{\alpha}{4\cdot\pi^2\cdot\omega}\gamma^2 \frac{e^{-R\cdot(1+X^2)^{1/2}}}{1+X^2+Y^2}\cdot[\cosh(2\cdot f\cdot\delta)-\sin(R\cdot Y+\Phi'(X,Y)],$$

$$\Phi'(X,Y) = \sin^{-1}[(1+X^2-Y^2)/(1+X^2+Y^2)] = \cos^{-1}[-2\cdot Y\cdot(1+X^2)^{1/2}/(1+X^2+Y^2)]$$

where :

- $\alpha = 1/137$ is the fine structure constant,
- r_σ and $r_\perp$ are the Fresnel reflection coefficients, considered here equal to unity,
- ω is the emitted photon pulsation, $\omega = \frac{2\cdot\pi\cdot c}{\lambda}$, $\bar{\lambda} = \frac{\lambda}{2\cdot\pi}$,
- δ is the displacement as shown in figure 1.a,

$$- \; R \equiv \frac{a}{\gamma\cdot\bar{\lambda}},$$

- is the wave vector, $k = 2\cdot\pi/\lambda$, $k_x = k\cdot\sin(\theta_x)$, $k_y = k\cdot\sin(\theta_y)$, $\theta_{x,y}$ are the projection angles of the vector $\vec{k}$ into the x,z and y,z planes respectively. $|\theta_{x,y}| \cong \gamma^{-1} << 1$,
- $X = \gamma\cdot\theta_x$, $Y = \gamma\cdot\theta_y$ are the x and y projected angles in units of γ^{-1},
- $f = \left[\bar{k}_x^{\,2} + \frac{\omega^2}{v^2\cdot\gamma^2}\right]^{1/2}$. A good approximation of $\cosh(2\cdot f\cdot\delta)$ for $\delta << a$ is given by

$$1 + 2\cdot\left(\frac{\delta}{\gamma\cdot\bar{\lambda}}\right)^2\cdot(1+X^2)$$

3.1 Data

For all the numerical applications made in paragraph 3 we use the following data:

- A frequency in the visible range namely $\nu = \omega/2\cdot\pi = 10^{15}$[rd.s^{-1}], then $\lambda=3.0\cdot10^{-7}$[m],
- a = 200μm, R = 0.1
- γ= 42000.0 so that $\gamma \cdot \bar{\lambda} = 2.10^{-3}[m]$.

Using these numbers we obtain:

$$C1 = (r_\sigma, r_\perp)^2 \cdot (\frac{\alpha}{4 \cdot \pi^2 \cdot \omega}) \cdot \gamma^2 = 5.19\cdot10^{-11}[\text{s}].$$

CLIC Parameters.

CLIC will operate from E_{min} = 9 GeV to E_{max} = 1.5 TeV. The transverse r.m.s. dimension σ and divergence σ' vary with energy E according to [3]:

$$\sigma_{h,v}(E) = \sigma o_{h,v} \cdot (\frac{E_{\min}}{E})^{1/4},\ \sigma'_{h,v}(E) = \sigma o'_{h,v} \cdot (\frac{E_{\min}}{E})^{3/4}$$

where $\sigma o_{h,v}$ and $\sigma' o_{h,v}$ are obtained from the electron beam normalized emittance in the horizontal and vertical planes.

Rough estimates for initial and final energies are given in Table 1.

Energy [GeV]	σ_h[m]	σ'_h[rad]	σ_v[m]	σ'_v[rad]	γ	1/γ	$\gamma \cdot \bar{\lambda}$
9	$1.6\cdot10^{-5}$	$1.98\cdot10^{-6}$	$2.13\cdot10^{-6}$	$2.66\cdot10^{-7}$	$1.8\cdot10^{4}$	$5.55\cdot10^{-5}$	$8.6\cdot10^{-4}$
1500	$4.4\cdot10^{-6}$	$4.26\cdot10^{-8}$	$6.0\cdot10^{-7}$	$5.74\cdot10^{-9}$	$3.0\cdot10^{6}$	$3.33\cdot10^{-7}$	0.143

Table 1

Considering the horizontal plane only, one sees that the slit aperture "a" could be about 200 μm. In such a case $R[E_{\min}] = 0.23$ *and* $R[E_{\max}] = 1.4\cdot10^{-3}$. For the remainder of this paper we have used $R = 0.1$ for numerical applications which corresponds to about 21.5 GeV.

We are using the projected angles in units of γ^{-1} (see par. 3). In the same way we must consider the divergence in units of γ^{-1} and therefore consider $\gamma\sigma'_h = 2.06\cdot10^{-2}(E[GeV])^{1/4}$ *and* $\gamma\sigma'_v = 2.22\cdot10^{-2}(E[GeV])^{1/4}$

4. Total intensity, Optical Set-up

The total intensity is the sum of the horizontal and vertical components:

$$N_t = \frac{d^2N}{d\omega d\Omega} = \frac{d^2N_{horiz}}{d\omega d\Omega} + \frac{d^2N_{vert}}{d\omega d\Omega}$$

Figure 2. represents a 3-D, and a contour plot of N_t (in arbitrary units concerning the amplitude; for the other parameters consult the legend).

The angular distribution can be recorded by using a lens. The object, or slit, is placed at the focal point of the lens while the detector is placed at infinity. The detector may consist of a CCD camera of which each pixel will record a light intensity having the distribution, in the X and Y plane identical to that given by Figure 2.

We now analyze in more details each polarization component of the emitted photon at a given frequency ω.

5. Influence of δ and of the Divergence on Polarization Components.

Each component can be disentangled from the total emitted radiation by the use of polarisers.

5.1 General Characteristics.

5.1.1 The Horizontal Component

$$N_h(X,Y,\delta) = \frac{d^2N_{horriz}}{d\omega d\Omega} = C1 \cdot \frac{X^2}{1+X^2} \frac{e^{-R\cdot(1+X^2)^{1/2}}}{1+X^2+Y^2} \cdot [\cosh(2\cdot f\cdot\delta) + \sin(R\cdot Y + \Phi'(X,Y)]$$

With: $C1 = (r_\sigma)^2 \cdot (\frac{\alpha}{4\cdot\pi^2\cdot\omega})\cdot\gamma^2$, $\delta << \gamma\cdot\bar{\lambda} \cong a$.

For some numerical applications, illustrated by Figures 3 to 8, we will take C1 = 1.

The function N_h has the following properties:

a) $N_h(X=0,Y,\delta) = 0$,
b) $N_h(X,Y,\delta) = N_h(\pm X,\pm Y,\delta)$

A 3-D plot of $N_h \equiv Mh$ is given in Figure 3 for the parameters mentioned in the legend. We can observe the properties and the symmetries given in a) and in b) above. The same distribution is represented in a contour plot form by Figure 4.a.

5.1.2 The Vertical Component.

$$N_v(X,Y,\delta) = \frac{d^2 N_{vert}}{d\omega d\Omega} = C1 \cdot \frac{e^{-R\cdot(1+X^2)^{1/2}}}{1+X^2+Y^2} \cdot [\cosh(2\cdot f\cdot\delta) - \sin(R\cdot Y + \Phi'(X,Y)]\,.$$

A 3-D plot of $N_v \equiv Mv$ is given in Figure 3 with the parameters given in the legend. We can observe the properties and the symmetries mentioned in a) and in b). The same distribution is represented, in the form of a contour plot, by Figure 4.b.

5.2) Influence of δ.

5.2.1 Horizontal Component.

We can proceed with a cut along the X-axis of Figure 4.a for Y =0.
A plot of $N_h(X,Y=0,\delta)$ for different values of δ, as a function of X, is shown in Figure 5.a. No significant influence of δ is observed. The difference is shown in Figure 5.b. Small but measurable differences are thus observed at the maximum of the nominal distribution. Again $N_h(X=0,0,\delta) = 0$ as mentioned in a previous paragraph.

In the case of a physical electron beam one has to consider a distribution of δ around δ_o with an r.m.s. spread $\Delta\delta$. The distribution can be expressed in a Gaussian form (when $\delta_o = 0$):

$$n(\delta,\Delta\delta) = n_o \frac{1}{\sqrt{2\cdot\pi\cdot\Delta\delta^2}} \exp(-\frac{\delta^2}{2\cdot\Delta\delta^2}) = n_o \cdot H(\delta,\Delta\delta)$$

where n_o is the total number of particles of interest (n_o is taken equal to unity in order to simplify our study). One must then proceed with a convolution product:

$$J_h(X,Y,\delta_o,\Delta\delta) = \int N_h(X,Y,\delta_o - u)\cdot H(u,\Delta\delta)\cdot du$$

As shown in Figure 5.a and .b the horizontal distribution $N_h(X,Y,\delta)$ is practically not influenced by δ<a and hence it is easy to prove that $J_h(X,Y,\delta_o,\Delta\delta) \cong N_h(X,Y,\delta)$. This is confirmed by a plot of $J_h(X,0,\delta_o=0,\Delta\delta=0.1\cdot a)$ and $N_h(X,0,\delta_o=0)$ in Figure 5.c and of their difference in Figure 5.d (to be compared with 5.b). This issue has been demonstrated in a previous paper [4].

5.2.2 Vertical Component.

Again let us proceed by taking a cut along the X-axis of Figure 4.b for Y = 0.
A plot of $N_v(X,0,\delta)$ as a function of X and different values of δ is given in Figure 6.a (notice that, according to 5.1.2, $N_v(X,0,0) = 0$). A plot of $N_v(0,Y,\delta)$ as a function of Y and for different values of δ is given in Figure 6.b while the detailed differences are given in Figure 6.c. Again the amplitudes of the differences are small with respect to that of the nominal distribution.

Considering now an electron beam distributed in position with an r.m.s spread Δδ the conclusions made in section 5.2.1 are also valid for the vertical plane.

5.3 Influence of the Divergence

5.3.1 Horizontal Component.

The effect of the velocity divergence in the horizontal plane, can be computed by considering a Gaussian distribution of the angle θ_x (or X) with r.m.s. "ε_p". One introduces a normalized angular distribution expressed by :

$$G_h(X,\varepsilon p) = \frac{1}{\sqrt{2\cdot\pi\cdot\varepsilon p^2}}\cdot e^{-\frac{X^2}{2\cdot\varepsilon p^2}}$$

The N_h distribution has now to be convoluted by G_h. The convolution product, for a given δ, is given by:

$$I_h(X,Y,\delta,\varepsilon_p) = \int_{-\infty}^{\infty} N_h(X-u,Y,\delta)\cdot G_h(u,\varepsilon p)du$$

$I_h(X,0,0,\varepsilon p=0.1)$ is shown in Figure 7.a together with $N_h(X,0,0)$. The main effect is that the distribution is no longer equal to 0 for X=0, showing up a direct effect of the divergence on the horizontal distribution along the X axis. In Figure 7.b we represent $I_h(X,0,0,\varepsilon p)$ for different values of εp

5.3.2 Vertical Component.

In the same spirit one can consider an angular distribution of θ_y (or Y) and define a corresponding angular spread δp. One introduces a Gaussian distribution:

$$G_v(Y,\delta p) = \frac{1}{\sqrt{2\cdot\pi\cdot\varepsilon p^2}}\cdot e^{-\frac{Y^2}{2\cdot\delta p^2}}$$

and convolute it with N_v. For a given δ we obtain the following expression:

$$I_v(X,Y,\delta,\delta p) = \int_{-\infty}^{\infty} N_v(X,Y-u,\delta)\cdot G_v(u,\delta p)du\ .$$

$I_v(0,Y,\delta,\delta p)$ is shown together with $N_v(0,Y,\delta)$ in Figure 8.a. It is easy to notice that the influence of the displacement δ and of the divergence δp are of the same order. In Figure 8.b we illustrate the influence of the divergence alone on the vertical distribution. The differences are significant.

5.3.3 Expected values for εp *and* δp

To the first order $\varepsilon p = \gamma\sigma'_h$ *and* $\delta p = \gamma\sigma'_v$
Using the numbers and equations obtained in paragraph 3, within the CLIC energy range

$$3.6\cdot 10^{-2} \le \varepsilon p = \gamma\sigma'_H \le 1.3\cdot 10^{-1}$$
$$3.85\cdot 10^{-2} \le \delta p = \gamma\sigma'_V \le 1.37\cdot 10^{-1}$$

Therefore the numbers used for εp and δp in Figures 7, 8 and 9 are consistent.

6. Interference's

In order to increase the emitted intensity, or enhance some other issues which could provide some improvements of the diagnostics, one could foresee an experiment making use of the interference between the forward radiation emitted by the upstream foils and the backward radiation emitted by the downstream foils. The interference intensity is expressed by [2]:

$$\frac{d^2N^I_{h,v}}{d\omega d\Omega} = \frac{d^2N^S_{h,v}}{d\omega d\Omega}\cdot \sin^2\left[\frac{\pi\cdot L}{2\cdot\lambda}\cdot(\gamma^{-2}+\theta^2_{x,y})\right]$$

where L is the distance between the foils, the superscript I (interference's) refers to the two slits and the superscript S refers to the single slit.
In order to have an interference pattern we must have:

$$\frac{\pi\cdot L}{2\cdot\lambda\cdot\gamma^2}\left[1+(\gamma\cdot\theta_{x,y})^2\right] = p\cdot\pi$$

where "p" is an integer. In our case $\gamma\cdot\theta_{x,y} = X,Y$ is of the order of a few units. An interference pattern supposes that p>1. Considering: p =1 = X and the values used for γ and λ we come to: $L > \lambda\cdot\gamma^2 = 530$m which practically is not acceptable.
Measurements using interference patterns could be foreseen for smaller γ's but not for CLIC.

7. Application to Beam Diagnostics

Classical diagnostics on an electron beam concerns the measurement of the mean position "δ", the beam divergence dδ and the beam transverse dimension. The use of the DR angular diffraction does not allow the measurement of the transverse beam dimension as such.

We have seen from Figure 5 that the horizontal component distribution is practically not influenced by the changes of "δ" and of "dδ". This is however not the case for the vertical component as explained in sections 5.2.2 and 5.3.2.

In this paragraph we therefore concentrate our interest on the vertical component where again we consider a cut along the Y axis for X =0.

7.1 Beam Position

A zoom of $I_v(0,Y,\delta,d\delta=0.1)$ is given in Figure 9.a, together with $N_v(0,Y,\delta=0)$. We see that for a given divergence, dδ = 0.1, a difference exists when δ= 0, a/4, and a/2. For Y = 0 the values are:

$$I_v(0,0,0,0,1) = 0.019,\ I_v(0,0,a/4,0,1) = 0.02,\ I_v(0,0,a/2,0,1) = 0.023.$$

The differences are very small and certainly difficult to detect since the noise level, at the minimum signal, has to be taken into account.

Theoretically, for a fixed dδ, the minimum at Y=0 is obtained for δ = 0. One can thus steer the beam so as to obtain a minimum and therefore centre the beam. Again practically the inherent noise has to be considered.

7.2 Beam Divergence

For a centered beam (δ = 0) a zoom of Figure 8.b is given in Figure 9.b. The influence of dδ is quite pronounced and seems usable for diagnostics.
One could for example integrate the signal along the line Y for X=0:

$$Sum(d\delta) = \int_{-Yo}^{Yo} I_v(0,Y,0,d\delta)\, dY$$

In the present case: Sum(0.1) = 1.677, Sum(0.2) = 1.673, Sum(0.4) = 1.656 for Yo =2.5. The differences are quite faint making such a technique practically unusable.
On the other hand one could measure the maximum and the minimum of I_v. In the present case (taking the maximum at Y = 1 and the minimum at Y = 0) we compute:

$I_v(0,1,0,0.09) = 0.494$, $I_v(0,0,0,0.09) = 0.015$, ratio = 32.93
$I_v(0,1,0,0.1) = 0.493$, $I_v(0,0,0,0.1) = 0.019$, ratio : 25.95,
$I_v(0,1,0,0.2) = 0.477$, $I_v(0,0,0,0.2) = 0.065$, ratio : 7.338,

$I_v(0,1,0,0.4) = 0.425$, $I_v(0,0,0,0.4) = 0.171$, ratio : 2.485.

The ratio varies significantly with dδ. Such a method could be foreseen to detect the variations in the beam divergence.

For example we have seen (5.3.3) that for CLIC "$d\delta$" is of the order of 0.1. If we foresee a 10% variation in divergence the effect is well illustrated by the above ratio differences when $d\delta = 0.09$ and $d\delta = 0.1$.

8 Conclusions.

The horizontal component of the DR angular distribution provides practically no way to make diagnostic measurements of the beam parameters.

On the other hand the vertical component should allow:

- A way to center the beam. The accuracy must however be checked.
- An accurate way to measure the beam divergence.

Of course another slit rotated by 90^o will allow us to measure the beam divergence in the horizontal plane.

In the case of high-energy beams ($\gamma >> 1$), as is the case for CLIC, the use of interferences is of no help.

References

[1] Diffraction Radiation Photon Yield. Preliminary studies in the frame of CLIC. J. Bosser, G. Tranquille, CLIC Note 546.

[2] Diffraction radiation diagnostics for moderate to high energy charged particle beams, R.B. Fiorito, D.W. Rule, NIM B 173 (2001) 67-82.

[3] Private Communication. E. D'Amico and G. Guignard.

[4] A new non-intercepting beam size diagnostics using diffraction radiation from a slit, M.Castellano, NIM A 394(1997) 275-280.

Figure 1. Geometrical data.

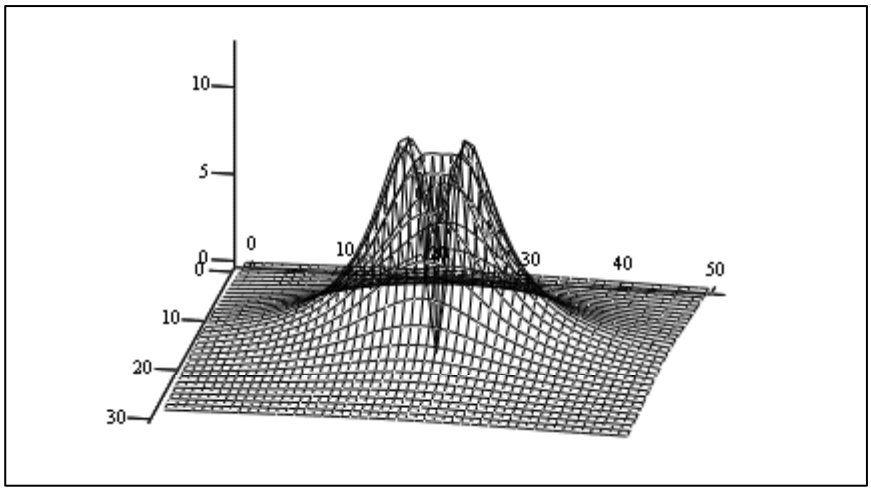

Mt

3-D Plot of the total Diffraction radiation angular spectral distribution Mt

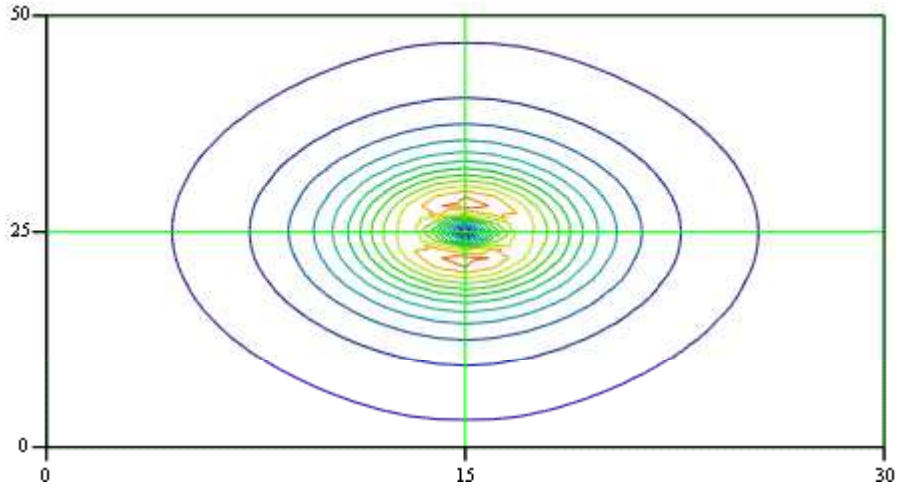

Mt

Contour plot of the total diffraction radiation distribution: Mt
x axis [0,Nmaxx] represents X= $\gamma . \Theta x$ from -bornex to bornex
y axis [0,Nmaxy] represents Y= $\gamma . \Theta y$ from -borney to borney

bornex = 7.5 borney = 7.5 R = 0.1 $\delta = 0$

Nmaxx= 30 Nmaxy = 50 coef = 25

Figure 2. Total diffraction radiation

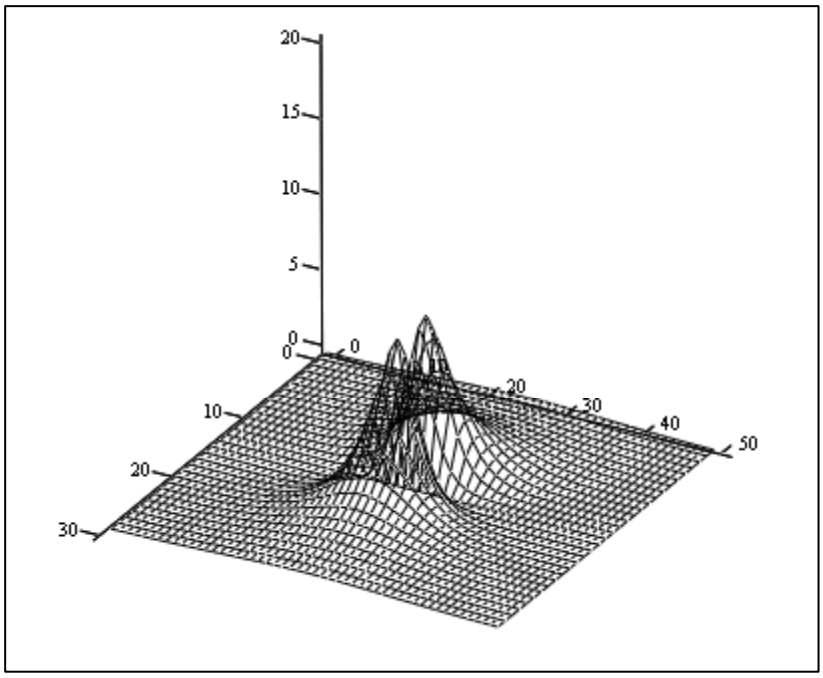

Mh

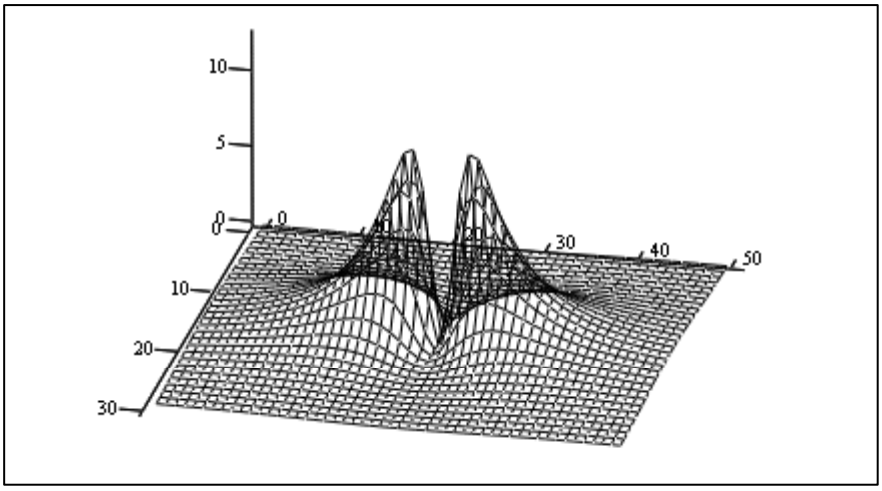

Mv

3-D plots of the horizontal distribution Mh and the vertical distribution Mv
x axis: [0,Nmaxx on the plot] represents X= $\gamma . \Theta x$ from -bornex to bornex
y axis: [0,Nmaxy on the plot] represents Y= $\gamma . \Theta y$ from -borney to borney
Amplitude multipled by coef

Nmaxx= 30 bornex = 7.5 Nmaxy = 50 borney = 7.5 coef = 25

R = 0.1 $\delta = 0$ $a = 2 \times 10^{-4}$

Figure 3 . Horizontal and vertical angular distributions

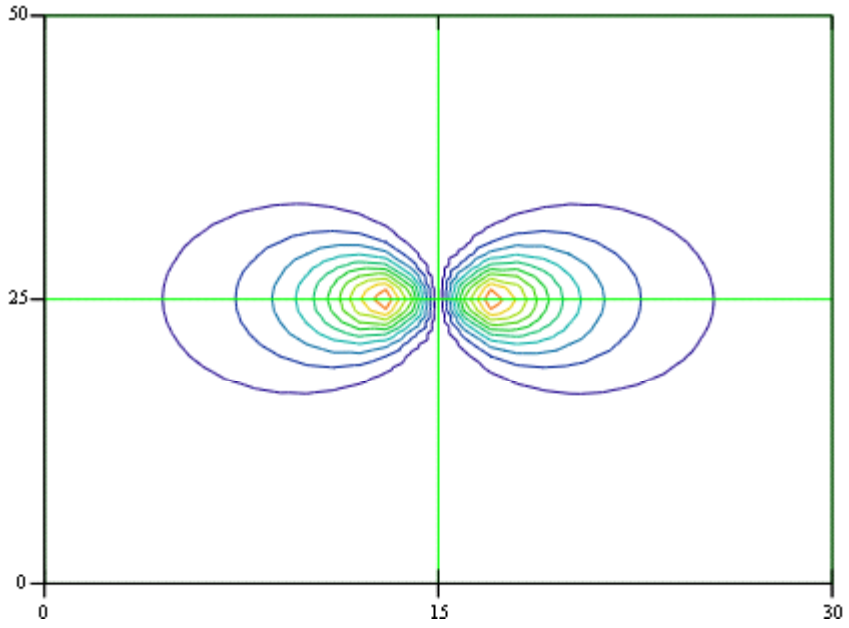

a)

(Mh)

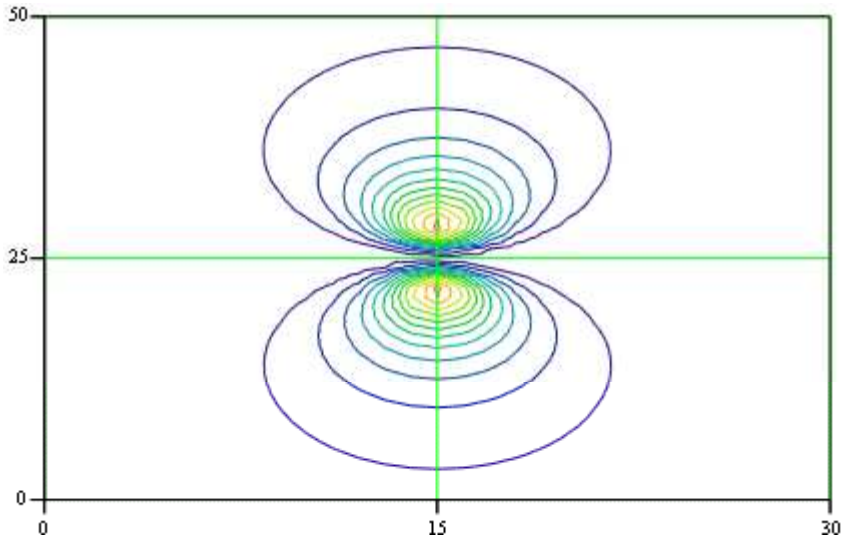

b)

Mv

Contour plots of the horizontal distribution Mh, vertical distribution Mv.
x axis [0,Nmaxx] represents X= $\gamma.\Theta$x from -bornex to bornex
y axis [0,Nmaxy] represents Y= $\gamma.\Theta$y from -borney to borney

bornex = 7.5 borney = 7.5 R = 0.1

Nmaxx= 30 Nmaxy = 50 δ = 0

Figure 4. Contour plots of the horizontal and vertical angular distribution

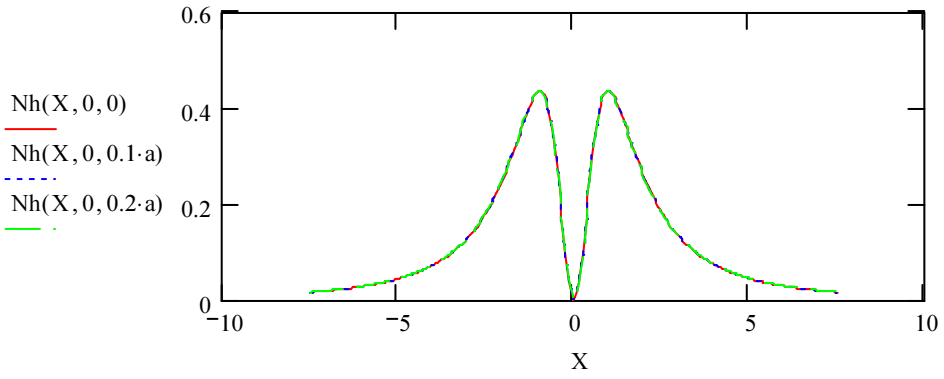

a)

Horizontaly polarized intensity Nh(X,Y, δ) versus X=γ.θx, Y=0, and different δ values.

$R = 0.1 \qquad a = 2 \times 10^{-4} \qquad \lambda b = 4.775 \times 10^{-8} \qquad \gamma \cdot \lambda b = 2.005 \times 10^{-3}$

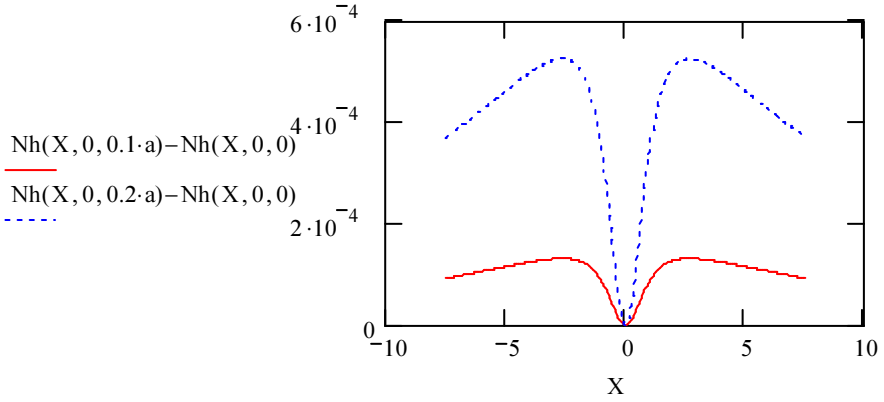

b)

Nh(X,0,δ)-Nh(X,0,0) for different values of δ

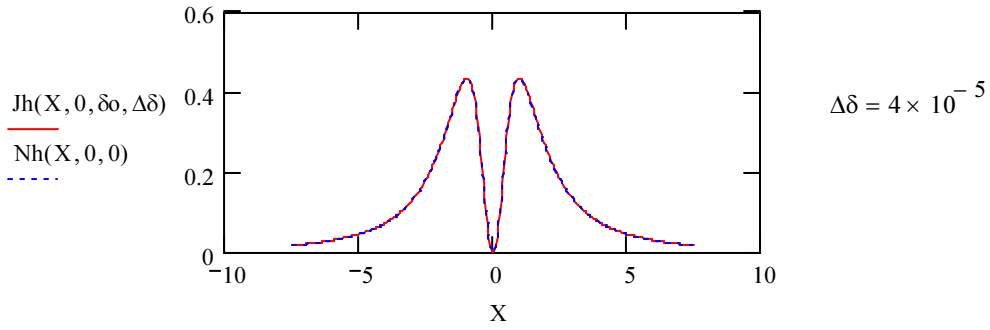

5.c) Convolution of the horizontal distribution with the spread on δ

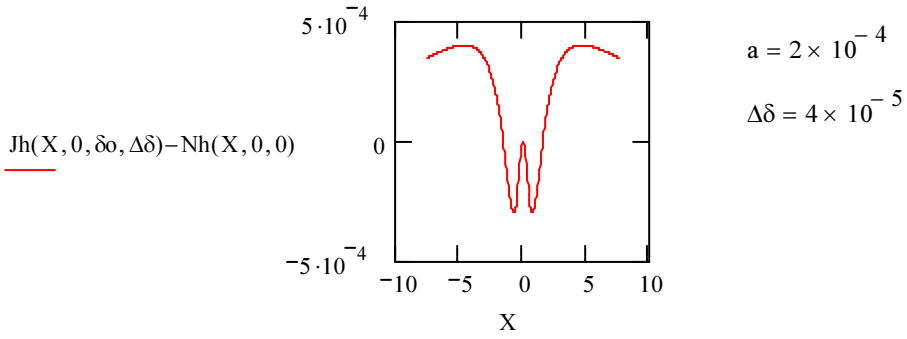

5.d) Difference

Figure 5

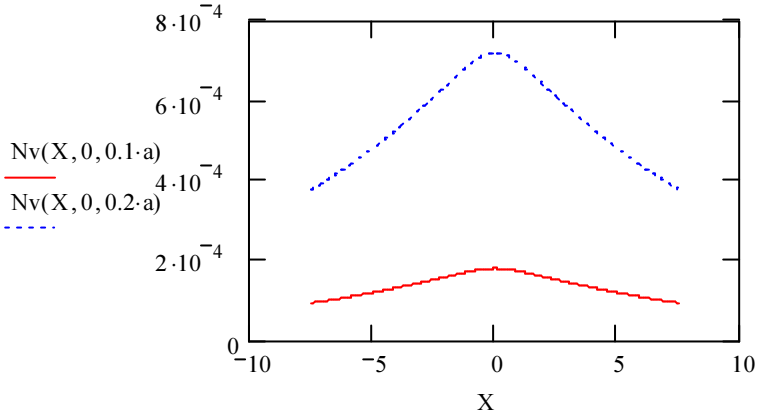

a)

Verticaly polarized intensity Nv(X,0,δ) versus X=γ.θx, Y=0.and different values of δ

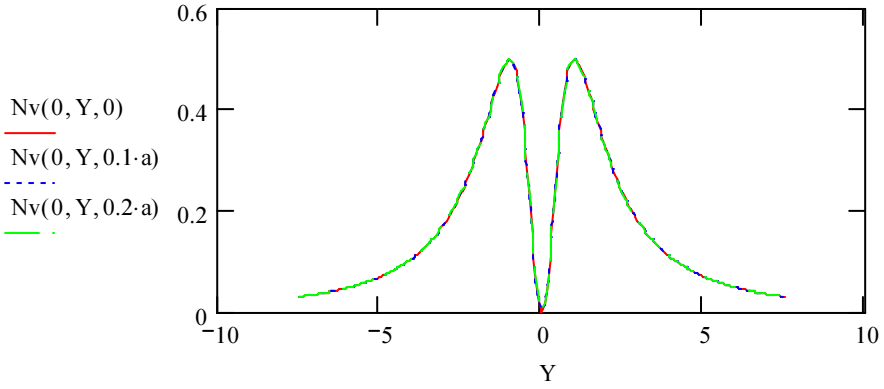

b)

Verticaly polarized intensity Nv(X,Y,δ) versus Y=γ.θy, X=0 and different δ

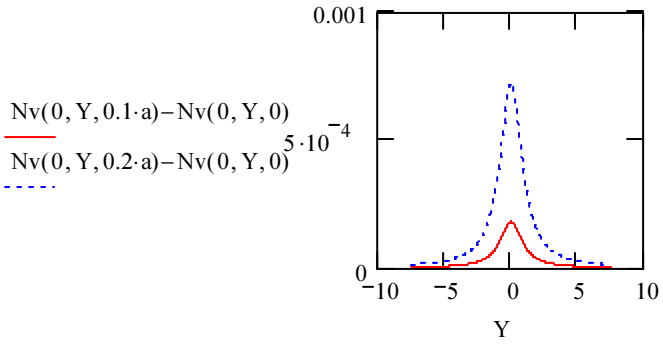

c)

Difference Nv(0,Yδ)-Nv(0,Y,0) for different values of δ

Figure 6 . Vertical polarisation analysis

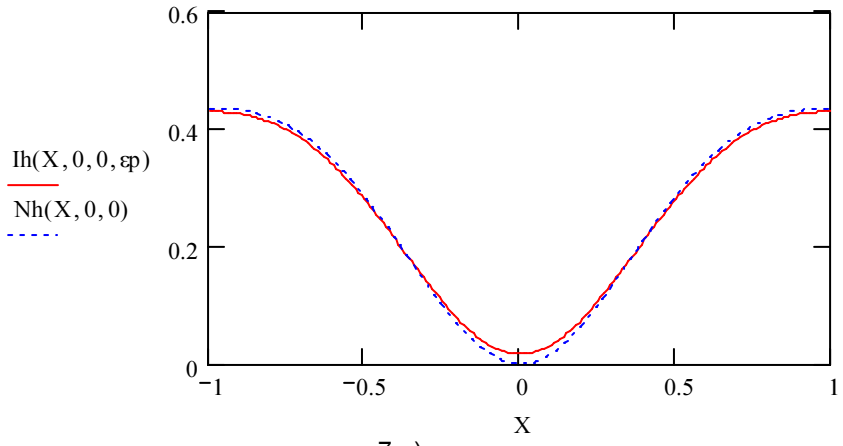

7.a)

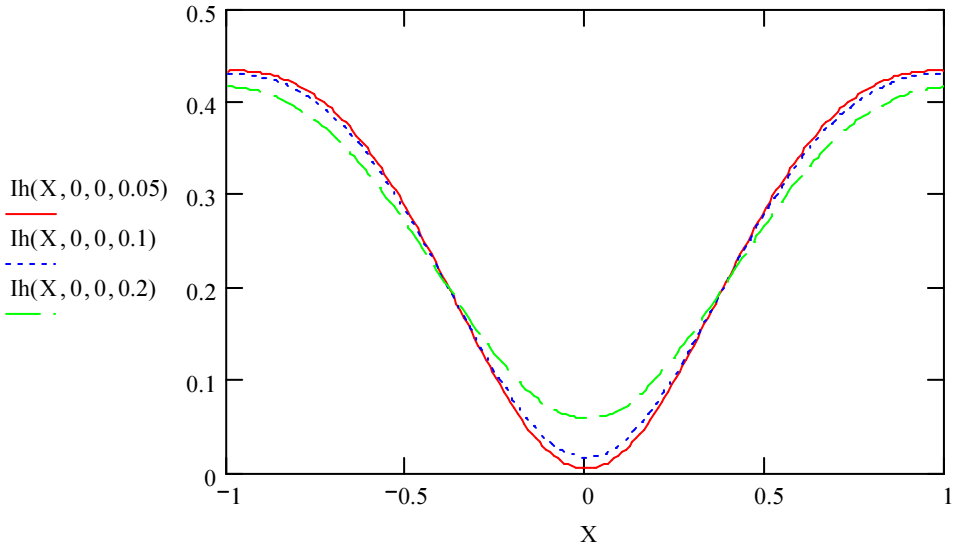

7.b)Effect of the divergenceδp on the horizontal intensity R = 0.1

Figure 7

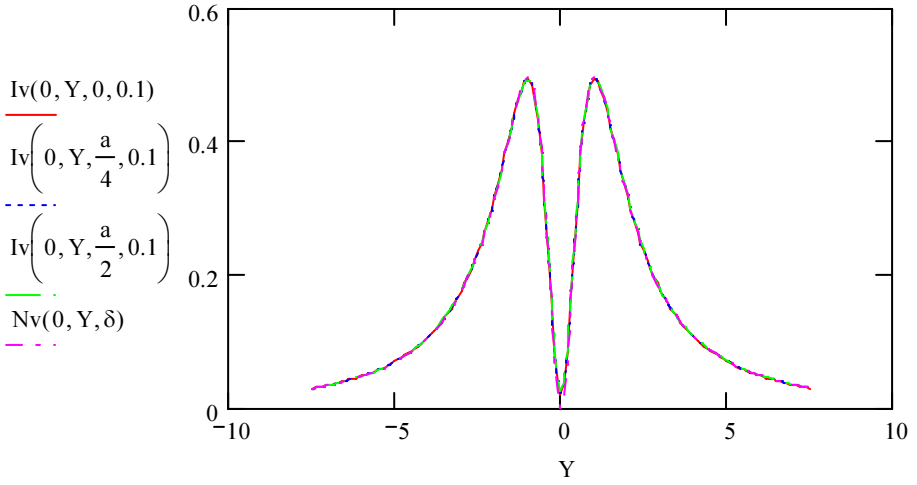

a)

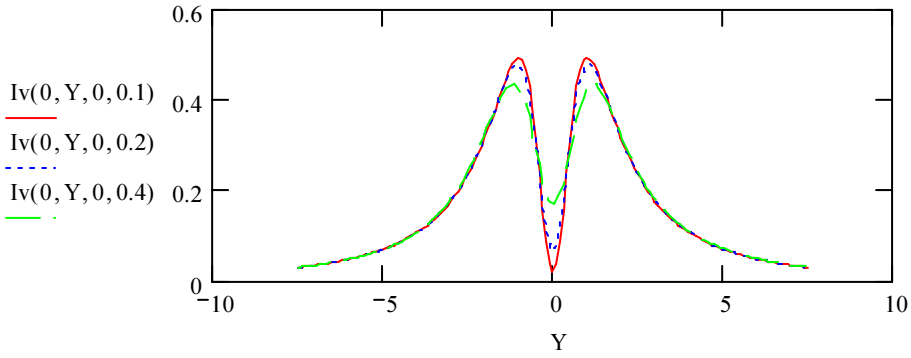

b)

Convolution of the vertical distributions with an angular distribution on Y

Figure 8.

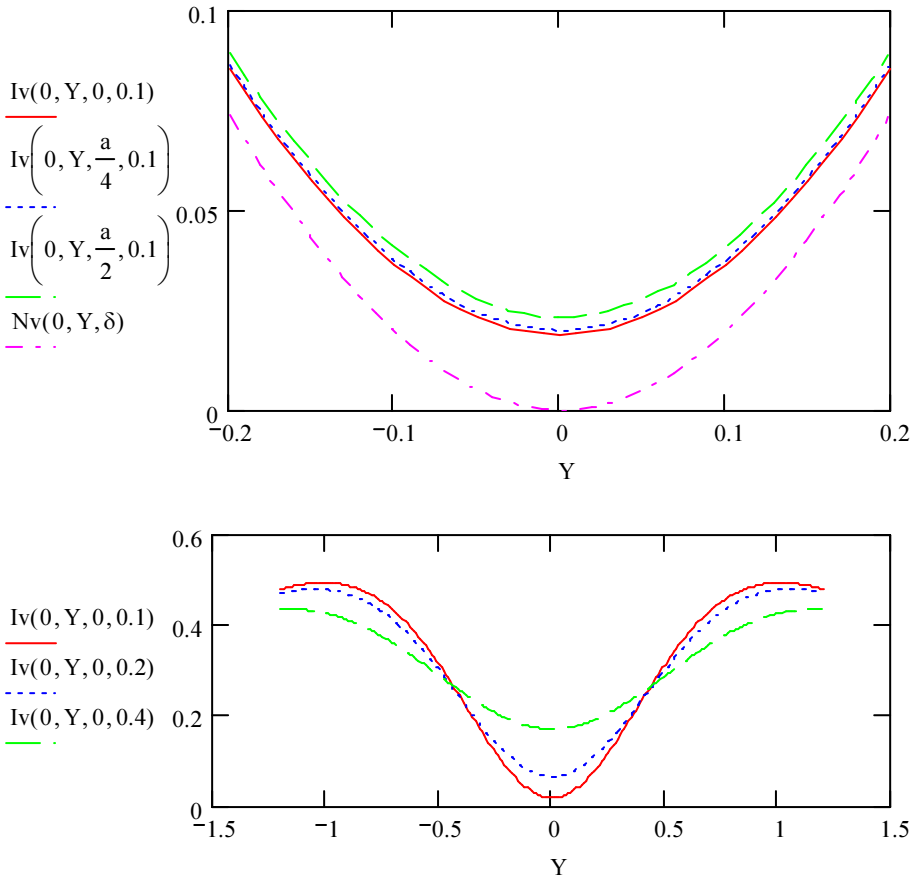

Convolution of the vertical distributions with an angular distribution on Y

Figure 9 . Zooming of figure 8